View metadata, citation and similar papers at core.ac.uk

brought to you by CORE

provided by Edinburgh Research Explorer

THE UNIVERSITY of EDINBURGH

Edinburgh Research Explorer

Performance Analysis of Virtual Carrier System Receivers for M2M Communications Using OFDMA

Citation for published version:
Wang, S & Thompson, J 2016, 'Performance Analysis of Virtual Carrier System Receivers for M2M Communications Using OFDMA' IET Communications, vol. 10, no. 16, pp. 2061-2070. DOI: 10.1049/iet-com.2015.1218

Digital Object Identifier (DOI):
10.1049/iet-com.2015.1218

Link:
Link to publication record in Edinburgh Research Explorer

Document Version:
Peer reviewed version

Published In:
IET Communications

General rights
Copyright for the publications made accessible via the Edinburgh Research Explorer is retained by the author(s) and / or other copyright owners and it is a condition of accessing these publications that users recognise and abide by the legal requirements associated with these rights.

Take down policy
The University of Edinburgh has made every reasonable effort to ensure that Edinburgh Research Explorer content complies with UK legislation. If you believe that the public display of this file breaches copyright please contact openaccess@ed.ac.uk providing details, and we will remove access to the work immediately and investigate your claim.

Download date: 05. Apr. 2019

Performance Analysis of Virtual Carrier System Receivers for M2M Communications Using OFDMA

Shendi Wang, John S Thompson, *Fellow, IEEE*,

Institute for Digital Communications, Joint Research Institute for Signal and Image Processing

School of Engineering, The University of Edinburgh, EH9 3JL, Edinburgh, UK

Email: Shendi.Wang@ed.ac.uk, John.Thompson@ed.ac.uk

Abstract

With increasing demand for Machine-to-Machine (M2M) communications, modifying existing Orthogonal Frequency-Division Multiple Access (OFDMA) communication systems, such as the Long Term Evolution (LTE) system, to successfully support low data rate M2M devices has became an important issue. In LTE Release 12 and beyond, the reduction of maximum bandwidth, the reduction of transmission power and the reduction of downlink transmission model should be studied for supporting low data rate M2M communications. This paper will address one solution based on the virtual carrier (VC) concept, which aims to improve the bandwidth efficiency and cost-efficiency, using analogue filters to extract only sub-carriers of interest. This will reduce the sampling rate at the M2M analog-to-digital converter (ADC) leading to improvements in ADC power consumption and the computational complexity. Our results indicate that the VC system can provide significant high signal-to-interference-plus-noise ratio (SINR) performance without significant Bit Error Rate (BER) degradation.

Index Terms

Virtual Carrier, Machine-to-Machine, OFDMA, Sampling Reduction, Aliasing, SINR.

I. Introduction

Wireless communication technologies have been rapidly developing in recent years, and mobile communication has become a basic tool for modern society. The current fourth generation (4G) networks, as known as the Long-Term Evolution (LTE) standards [1], it provides high spectrum efficiency by combining advanced multi-antenna techniques and implements the orthogonal frequency division multiple access (OFDMA) scheme in the downlink (DL) from the base station to the mobile terminals. In terms of supporting synchronisation, LTE uses a subset of carriers to transmit downlink control information (DCI) in the physical downlink control channel (PDCCH) [2]. With increasing the number of PDCCH, the sub-carrier efficiency will decrease. Projections for the growth machine type communication (MTC) devices range up to 50 billion in the next few decades, compared to the 2 billion devices which are directly connected to the wireless communication network [3]. The communication network will shift from the existing Human to Human (H2H) communication mode to the Machine to Machine (M2M) communication mode.

A. Motivation and Related Work

With the growth of automated systems such as e-health, the smart grid, smart homes and smart cites, M2M communications will experience exponential growth in the next generation of mobile communication systems [4]. M2M communications is one of the most promising solutions for revolutionising [5] future intelligent wireless applications. The major idea of M2M communication system is allowing M2M terminal devices or components to be interconnected, networked, and controlled remotely [6], with the advantages of low-cost, scalable and reliable technologies.

One of the major challenges for supporting M2M communications using LTE is how to reduce the processing cost to maximum the battery life of M2M terminal devices. For instance, the LTE downlink channel can provide up to 20 MHz bandwidth. However, M2M communications usually require low data rate transmission, for instance, an M2M terminal device may only be allocated 1MHz out of the 20MHz LTE downlink channel. In this case, most of the sub-carriers are not relevant to the M2M device. Therefore, how to reduce the energy and processing cost of LTE in order to support M2M low cost devices with increasing the bandwidth efficiency will be a major issue for standardisation beyond Release 12 of LTE [2]. This paper will study how reduced sampling rates in M2M receiver devices can improve their energy efficiency without losing performance.

To the best of our knowledge, there are no previous works which studied reducing the LTE bandwidth in order to support low data rate M2M communications. Reference [7] only proposes a possible solution: insert a M2M low data rate message into the LTE downlink channel and design a Virtual Carrier (VC) to contain the message. This VC can be separately scheduled to support low bandwidth M2M devices and the remaining sub-carriers are designed to support high data rate services as normal. However, reference [7] did not describe a detailed system structure nor how to extract the low data rate virtual carrier messages at the receiver.

B. Contributions

Considering the LTE downlink capacity, we reduce the analogue-to-digital converter (ADC) costs and computational complexity by reducing the sampling rate. Our main contributions are as follows:

1) Propose a novel reduced sample rate VC receiver system. Compared with the current LTE carrier aggregation technique, it significantly improves the bandwidth efficiency.

2) The VC system significantly reduces the ADC cost and computational complexity while providing high Signal-to-Interference-and-Noise Ratio (SINR) and low Bit Error Rate (BER) performance to support low data rate M2M devices.
3) Drive a closed-form expression for SINR which includes the additional interference caused by aliasing effects. Our previous study [8] shows that aliasing effects caused by the filter and the lower sampling rate ADC can reduce the VC system performance. Firstly, our SINR analysis includes the effect of the filter cut-off frequency, the receiver ADC sampling rate and the sampling reduction ratio. Secondly, the BER can also be evaluated in closed from to show the trade-off between system parameter choices and detection performance.
4) Drive a closed-form expression for the effect of inter symbol interference (ISI) caused by asynchronism. We also consider several cases, including: very dispersive multipath channel effects on ISI and inter carrier interference (ICI) plus the additional interference caused by sample timing errors.

The rest of this paper is organised as follows: Section II introduces the state of the art. We discuss the VC receiver system model and derive the performance analysis in Sections III and IV, respectively. The LTE bandwidth efficiency and analytical results comparing with different SINR and BER performance are shown in Section V and Section VI concludes the paper.

II. OFDM System: State of The Art

This section will provide a brief introduction of the standard OFDM transmitter and receiver and introduce three options to support reduced bandwidth transmissions in OFDMA for M2M devices.

A. Standard OFDM System

1) Transmitter For OFDM: Orthogonal frequency division multiplexing inherently provides good protection against ISI due to the long symbol cyclic prefix (CP), where the length of CP in samples is defined as L_{CP} , and it is used in cellular systems such as LTE and WiMAX [9]. Assume that the message bits are to be transmitted using OFDM modulation with N sub-carriers. Denote the frequency domain symbols by $X_m, m = 0, 1, ..., N-1$. Then, the baseband signal for an OFDM symbol can be expressed as:

$$x(t) = \frac{1}{N} \sum_{m=0}^{N-1} X(m) \cdot e^{j2\pi mt/N} (m = 0, 1, ..., N-1), \tag{1}$$

where $X(m)$ is the fast Fourier transform (FFT) of x. The signal $x(t)$ is up-converted to radio frequency, transmitted and propagates through the wireless channel.

2) Model For the Standard OFDM Receiver: The transmitted signals will go though a wireless channel and the impulse response can be modelled as:

$$h_i = \sum_{j=0}^{J-1} h_{ij} \delta(t - jT_{\mathrm{s}}), \tag{2}$$

where i is the time index, and each channel tap h_{ij} follows the Rayleigh distribution, T_{s} is the sample period, and $\delta(t)$ is the Dirac delta function. (For the additive white Gaussian noise (AWGN) channel without multipath, $J = 1, h_{ij} = 1$.) The received signal over the Rayleigh multipath channel and AWGN channel can be defined as $y(t)$:

$$y(t) = x(t) \otimes h_i + g_{\mathrm{o}}(t), \tag{3}$$

where $\otimes$ denotes the convolution operation and $g_{\mathrm{o}}(t)$ represents AWGN with power spectral density $N_0/2$ is assumed. For a standard OFDM receiver as shown in Fig. 1(a), the received signal is match filtered and sampled at frequency f_{s}. After removing the CP and applying the

FFT, the frequency domain signal can be expressed as:

$$Y(m) = X(m) \cdot H(m) + G_{\mathrm{o}}(m), \tag{4}$$

where $H(m)$ is the FFT of the vector [h_{i0}, h_{i1},..., h_{iJ-1}] and G_{o} is the FFT of the noise sequence g_{o} in the frequency domain. Finally, to decode the transmitted messages, zero forcing equalisation [10] can be used to estimate the transmitted data.

B. Options to Reduce OFDMA Bandwidth For M2M Devices

In order to support low data rate communications, the maximum bandwidth of OFDMA systems such as LTE should be reduced. Reference [7] lists three possible solutions, including separate carrier (SC), carrier aggregation (CA), and virtual carrier (VC).

1) Separate Carrier : The easiest way to reduce the maximum bandwidth is to separate a high bandwidth carrier into several narrower band carriers to support low bandwidth M2M devices. For instance, a 20MHz bandwidth carrier can be split into several 1.4MHz and 3MHz carriers. Low bandwidth M2M devices transmit and receive messages on each separate carrier and all narrow bandwidth M2M devices share the same OFDMA channel. However, the SC option will no longer support full bandwidth 20 MHz data transmissions and data capacity will be limited by the maximum bandwidth carrier.

2) Carrier Aggregation : One of the key features for LTE-Advanced is the carrier aggregation technique [11]. It allows a user equipment (UE) to receive data on multiple carriers simultaneously. In order to support low data rate M2M communication devices in LTE, one 20 MHz band can be formed by component carriers of bandwidth 1.4 MHz, 3 MHz, and 15 MHz. The low bandwidths support M2M communications, and the high bandwidth carriers such as 15 MHz can

support high data rate transmissions. However, CA does not improve the bandwidth efficiency, as each sub-band still needs several carriers to support synchronisation of the downlink channel.

3) Virtual Carrier: Here the transmitter insets a virtual carrier to carry the M2M messages into a 20 MHz downlink OFDMA channel to support low cost devices. High data rate devices can still use the remaining carriers.

In Section V, it will be shown that compared with SC and CA, by using a virtual carrier mapped into a 20 MHz band the transmitter obtains the highest bandwidth efficiency but the receiver ADC power cost reduces linearly with reduced sampling rate. In the following sections, this paper will study the VC receiver system in detail.

III. The Virtual Carrier System

This section will introduce the proposed VC receiver system then analyse the LTE downlink efficiency and the ADC energy cost performance. We assume that the filter information has been transmitted through the PDCCH channel to each terminal devices.

A. Sub-sampling Receiver for VC Option

In order to improve OFDMA bandwidth efficiency, this paper studies a novel receiver system supporting M2M communications. The principle of the VC receiver is shown in Fig. 1 (b). With the assumption that the standard OFDMA receiver received a set of messages over a 20 MHz channel bandwidth, the signal will pass through a 20 MHz analogue circuit filter and then be passed to an ADC with a higher sampling rate, e.g. 30.72 MHz as in LTE. Unlike the traditional OFDMA receiver, the major feature of the VC receiver system is improving the bandwidth efficiency by integrating both low data rate M2M messages and high data rate wideband messages in one downlink channel. M2M receivers can reduce the ADC processing cost

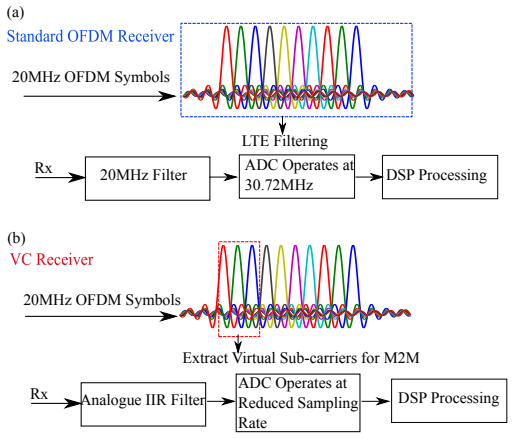

Fig. 1. (a) Standard LTE Receiver and (b) VC System Receiver.

by reducing the receiver's bandwidth to capture only the M2M sub-carriers of interest and filter out other sub-carriers. Therefore, a VC receiver implements one or more narrow band infinite impulse response (IIR) filters to extract the transmitted M2M signals from the received OFDMA signal. It operates the ADC at a much lower sample rate to reduce the power consumption and the number of subsequent digital signal processing computations to decode the signal. The scenario where an M2M receiver has received a 20 MHz bandwidth LTE signal but only a few sub-carriers (e.g. 70 carriers) are used for this terminal device is shown in Fig. 1 (b). A standard 20 MHz LTE bandwidth maps to a fast Fourier transform (FFT) size of 2048 with a sampling rate of 30.72 MHz. Therefore, the useful sub-carrier rate R_{U} for the M2M device can be calculated as the number of VC sub-carriers (70) divided by the total number of sub-carriers (2048), which is approximately $1/32$ in this case. Thus, a 0.625 MHz low pass filter (LPF) can be designed to extract the relevant sub-carriers from the 20 MHz bandwidth signal. A correspondingly lower sampling rate ADC is used at the low pass filter (LPF) output; in this case, we can choose a 0.96 MHz sampling frequency ADC instead of 30.72 MHz.

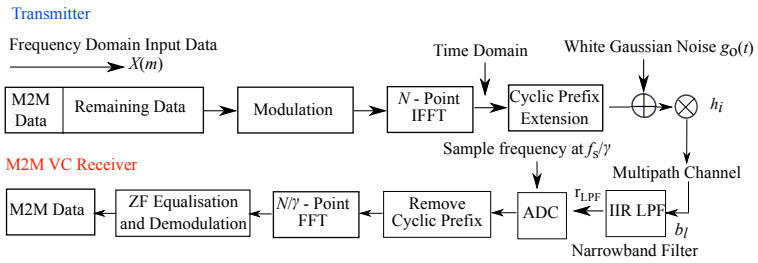

Fig. 2. Block Diagram of the VC Receiver System.

B. Mathematical Model of the VC Receiver

The VC receiver block diagram is shown in Fig. 2. The major function of the VC receiver system is to demodulate only sub-carriers of interest. Therefore, the major difference of the VC receiver compared to a standard OFDM receiver is that the received signals are passed to a narrowband IIR filter which separates the virtual carriers from the rest of the OFDM sub-carriers, then samples those carriers using a much lower sample frequency ADC. In order to determine the SINR performance, the narrowband IIR filter can be approximately expressed as an finite impulse response (FIR) filter with the impulse response written as b_l with length of $L_{\rm F}$. Denote the composite effect of the multipath channel and the IIR filter by $w_{\rm cn}(t)$:

$$w_{\rm cn}(t) \approx h_i \otimes b_l = \sum_{z=0}^{Z-1} w_{\rm cn}(z)\delta(t - zT_{\rm s}), \tag{5}$$

where, Z is the length of the combined channel impulse response. In the rest of paper, every the combined filter is approximated as being FIR. The received signal after an IIR filter can be designed as $r_{\rm LPF}$:

$$r_{\rm LPF}(t) = \{x(t) \otimes h_i + g_{\rm o}(t)\} \otimes b_l = x(t) \otimes w_{\rm cn}(t) + g'_{\rm o}(t) + i_{\rm A}(t) + q(t). \tag{6}$$

Equation (6) shows that the receiver filter b_l may increase the delay spread of the channel filter h_i. The scalar $i_A(t)$ is the aliasing noise (due to the effect of the narrow band filter and the reduced

sample rate processing) and $q(t)$ is the quantisation noise. For a realistic system, the effect of uniform quantisation can often be modelled by an additive noise term due to quantisation noise, which is uncorrelated with the input signal and has zero mean and a variance of $q^2/12$, where q is the quantisation step size [12]. In order to simplify the analysis results, this paper will assume that the aliasing effect dominates over the quantisation noise. Transforming w_{cn} into the frequency domain yields the following expression for the frequency response of sub-carrier m:

$$W_{\mathrm{cn}}(m) = \sum_{n=o}^{Z-1} w_{\mathrm{cn}}(n) \cdot e^{-j2\pi mn/N}. \tag{7}$$

In terms of reducing the ADC cost and the number of subsequent digital signal processing computations, the VC receiver system employs a much lower sampling rate f_{vc} rather than the standard sampling rate f_{s}, thus the sampling reduction ratio γ can be defined as:

$$\gamma = \frac{f_{\mathrm{s}}}{f_{\mathrm{vc}}}. \tag{8}$$

With the effect of the analogue IIR filter and reduced sampling rate ADC, the number of operating sub-carriers has been reduced to $K = N/\gamma$, which means the VC receiver FFT size is reduced to N/γ. Assuming that the length of the CP in samples is longer than combined channel and filter response, and the signal is sampled with the correct timing, the received M2M signal in the frequency domain after CP is removed can be denoted as:

$$R(k) = \beta \cdot X(k) \cdot W_{\mathrm{cn}}(k) + \beta \cdot G_{\mathrm{o}}(k) + I_{\mathrm{A}}(k) \quad (k = 0, 1, ..., N/\gamma - 1). \tag{9}$$

Where I_{A} is the aliasing term and the term β is the scaling mismatch factor between the transmitter and the receiver and reflects the different sample rates and FFT sizes at these two devices. Given that this scaling mismatch factor affects both the signal and the noise equally, then we can neglect it and assume $\beta = 1$ without loss of generality. The transmitted M2M signal

in the frequency domain $\hat{X}(k)$ can be estimated using zero forcing equalisation as:

$$\hat{X}(k) = \frac{R(k)}{W_{\mathrm{cn}}(k)}. \tag{10}$$

C. LTE Downlink Efficiency

The LTE downlink bandwidth directly relates to the overall transmission efficiency of the system as this determines the proportion of data sub-carriers in a radio frame. In the LTE downlink channel, in terms of providing good signal synchronisation performance, it uses several synchronisation Channels such as the Primary Synchronisation Channel (PSCH), the Secondary Synchronisation Channel (SSCH) and the PDCCH channel. However, those synchronisation channels will share lots of sub-carriers. In order to estimate the LTE downlink channel bandwidth efficiency, the percentage capacity of the LTE FDD (frequency division duplex) downlink channel is computed as:

$$C = \frac{N_{\mathrm{A}}}{N_{\mathrm{T}}} \cdot 100\%, \tag{11}$$

where we assume that a 10 ms radio frame is divided into 20 equal size slots of 0.5 ms [13]. A subframe consists 2 consecutive slots, therefore one 10 ms radio frame contains 10 subframes. C is the capacity of one 10 ms LTE FFD radio frame, N_{A} is the number of available sub-carriers and N_{T} is the number of total occupied sub-carriers in one frame, which can be computed from reference [14]. The standard LTE downlink channel bandwidth is 1.4 MHz, 3 MHz, 5 MHz, 10 MHz, 15 MHz or 20 MHz.

D. Synchronisation for the VC System

As mentioned above, cell synchronisation is the very first step when an M2M device wishes to connect to a cell. LTE users first find the primary synchronisation signal (PSS) [2] which is

located in the last OFDM symbol of first time slot of the first subframe as shown in Fig. 3. This enables users to be synchronised at the subframe level. In the next step, the terminal finds the secondary synchronisation signal (SSS) which determines the physical layer cell identity group number. In order to decode the VC message, a VC control signal (VCCS) should be included in the VC carrier as shown in Fig. 3. The VCCS includes the VC carrier locations, filter parameters and sampling reduction ratio. When the VCCS has been decoded, the M2M terminal devices can easily decode the received signals intended for it. The VCCS can be also mapped into the VC carrier to assist the M2M receiver in maintaining accurate symbol timing. The VC system decoding processing as below:

Processing 1 ***VC Synchronisation Steps***

Step 1: Search for the PSS and the SSS

Step 2: Decode the VCCS to identify VC carrier location

Step 3: Set filter parameters and receiver sampling rate

Step 4: Decode received M2M messages from the specified VC location

E. Energy Saving For The VC Receiver

The basic motivation for the VC system is the fact that for an ADC, the power dissipation is a linear function of the sampling rate. A previous study [15] derived the power dissipation of an ADC as P_{o},

$$P_{\mathrm{o}} = 48 k_{\mathrm{B}} T_{\mathrm{Temp}} \cdot 2^{2V} \cdot f_{\mathrm{s}}, \tag{12}$$

where k_{B} is Boltzmanns constant, T_{Temp} is temperature, f_{s} is the sampling frequency and V is the SNR-bits, which is given by [15]:

$$V = \frac{\mathrm{SNR[dB]} - 1.76}{6.02}. \tag{13}$$

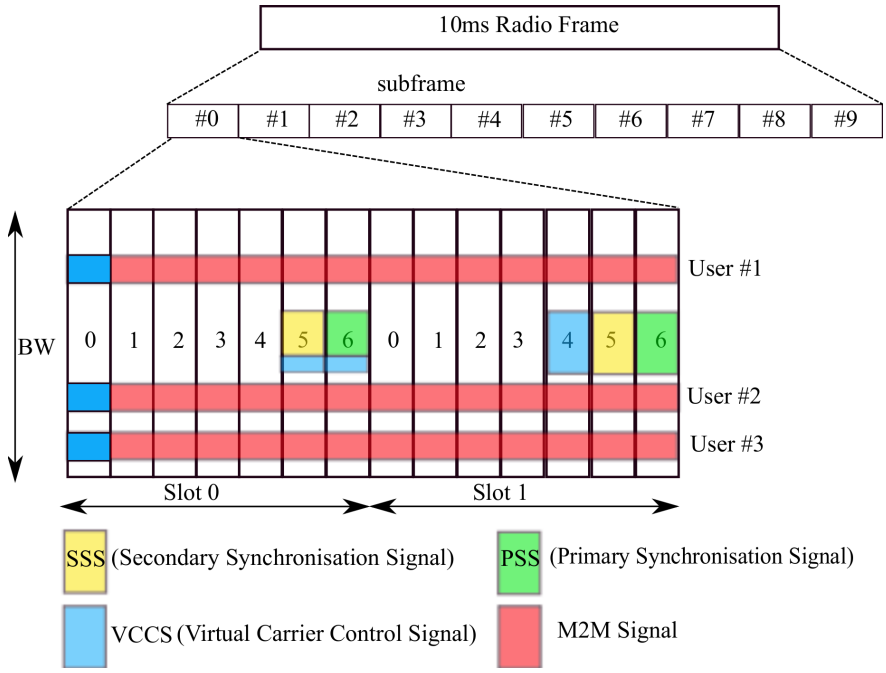

Fig. 3. Virtual Carrier Synchronisation Signals

Therefore, the ADC power dissipation presents a linear reduction by reducing the sampling frequency.

In terms of the FFT computational complexity, compared with the standard OFDM system, the VC receiver also reduces the number of subsequent digital signal processing computations. The computational complexity for the standard OFDM receiver C_{OFDM} can be defined as [16]:

$$C_{\mathrm{OFDM}} = \frac{N}{2} \cdot \log_2 N, \tag{14}$$

where N is the size of FFT for the original OFDM receiver. In terms of the VC receiver system, the received M2M low data rate messages after filtering with a lower sampling rate ADC, the FFT size can be decreased to N/γ. Therefore, the computational complexity for the VC receiver system can be defined as:

$$C_{\mathrm{VC}} = \frac{N/\gamma}{2} \cdot \log_2 (N/\gamma). \tag{15}$$

IV. Performance Analysis

In terms of computing the overall SINR performance of the VC receiver system, this paper will focus on three distinct channel scenarios to evaluate system performance. This paper will not consider the effect of time or frequency offset, thus, we make the assumption of the perfect sampling timing.

A. No Channel Effect SINR Analysis

Firstly, we evaluate a simple scenario, in order to evaluate only the effects of filter aliasing in $i_{\mathrm{A}}(t)$, which is computed by the analogue filter response and the reduced sampling rate ADC in the VC receiver (See Fig.2). We assume the received M2M message $y_{\mathrm{F}}(t)$ is not corrupted by background noise ($G_{\mathrm{o}} = 0$) or multipath channel effects. The received signal can be expressed as:

$$y_{\mathrm{F}}(t) = x(t) \otimes b_i(t). \tag{16}$$

With the assumptions of perfect sampling timing, a sampling reduction rate of γ and the case that the CP duration is longer than filter impulse response $b_i(t)$, then we can write down an expression for the FFT output of $y_{\mathrm{F}}(t)$, after the CP is removed. The m-th frequency bin can be denoted as [17]:

$$y_{\mathrm{F}}(m) = \sum_{n=0}^{N-1} X(n) \cdot B(n) \cdot e^{-j2\pi nm/K} = \sum_{k=0}^{K-1} \left(\sum_{a=0}^{\gamma-1} X(aK+k) \cdot B(aK+k) \right) \cdot e^{-j2\pi km/K}, \tag{17}$$

where $B(n)$ is the n-th bin of the Fourier transform of the filter impulse response b_i. Therefore, the received k sub-carrier signal after reducing the sampling rate in the frequency domain can be written as:

$$R_{\mathrm{F}}(k) = \sum_{a=0}^{\gamma-1} X(aK+k) \cdot B(aK+k). \tag{18}$$

After reducing the sampling rate at the receiver, there are γ copies of the original OFDM signal centred at frequencies 0, $f_{\rm s}/\gamma, 2f_{\rm s}/\gamma, ..., (\gamma-1)f_{\rm s}/\gamma$. The 0 frequency term is the desired spectrum of the transmitted signal $x(t)$ while the remaining frequencies represent undesired aliased components. Thus, equation (18) can be re-written as:

$$R_{\rm F}(k) = X(k) \cdot B(k) + \sum_{a=1}^{\gamma-1} X(aK+k) \cdot B(aK+k), \tag{19}$$

the aliasing term can be expressed as:

$$I_{\rm A}(k) = \sum_{a=1}^{\gamma-1} X(aK+k) \cdot B(aK+k), \tag{20}$$

and it represents all the aliased interference present in the received signal.

The SINR value for the signal can be computed as:

$$SINR(k) = \frac{\mathrm{E}[S(k)^2]}{\mathrm{E}[N_{\rm I}(k)^2]}, \tag{21}$$

where $\mathrm{E}[\cdot]$ denotes statistical expectation, $S(k)^2$ is the received signal power over at the output of the IIR filter, and $N_{\rm I}(k)^2$ is the interference power arising from the $(\gamma-1)$ aliased terms. Thus, the interference power for no channel effect case $N_{\rm IF}$ can be written as:

$$\mathrm{E}[N_{\rm IF}(k)^2] = \mathrm{E}\left[|R_{\rm F}(k) - X(k)\cdot B(k)|^2\right] = \sum_{a=1}^{\gamma-1} \mathrm{E}\left[X(aK+k)^2\right] \cdot |B(aK+k)|^2 . \tag{22}$$

Thus, the theoretical SINR value at the output of the VC receiver without channel effects can be derived as:

$$SINR_{\rm F}(k) = \frac{\mathrm{E}\left[X(k)^2\right] \cdot |B(k)|^2}{\sum_{a=1}^{\gamma-1} \mathrm{E}\left[X(aK+k)^2\right] \cdot |B(aK+k)|^2}. \tag{23}$$

B. AWGN Channel Effect SINR Analysis

Assume now the transmitted M2M signals go through an AWGN channel where the noise has mean zero and a noise standard deviation of $\sigma = \sqrt{f_{\rm s} N_0/2}$. Similar to equations (4), (19), the

received M2M messages from the AWGN channel in the frequency domain can be expressed as:

$$R_{\mathrm{A}}(k) = X(k) \cdot B(k) + \sum_{a=1}^{\gamma-1} X(aK+k) \cdot B(aK+k) + G_{\mathrm{o}}(k). \tag{24}$$

Thus, the theoretical SINR value of VC receiver at k sub-carrier for the AWGN channel can be derived as:

$$SINR_{\mathrm{A}}(k) = \frac{\mathrm{E}\left[X(k)^2\right] \cdot |B(k)|^2}{\sigma^2 + \sum_{a=1}^{\gamma-1} \mathrm{E}\left[X(aK+k)^2\right] \cdot |B(aK+k)|^2}. \tag{25}$$

C. Multipath Channel SINR Analysis

This section is devoted to address the effect of multipath channels by analysing the combined impulse response w_{cn} of both the multipath Rayleigh channel and the analogue filter in equation (5). We consider two cases when the length of combined response is both longer and shorter than the CP length in samples.

1) CP Longer Than Combined Response: Assume that a M2M receiver has received the signals over a Rayleigh multipath channel and an IIR filter has been applied at the receiver. The cyclic prefix length L_{CP} is longer than the combined response and we assume the received signal is sampled with the correct timing. According to equations (7), (17), the received signal in the frequency domain can be expressed as:

$$\begin{aligned} y_{\mathrm{Lo}}(m) &= \sum_{n=0}^{N-1} X(n) \cdot W_{\mathrm{cn}}(n) \cdot e^{-j2\pi nm/K} + g(m) \\ &= \sum_{k=0}^{K-1} \left(\sum_{a=0}^{\gamma-1} X(aK+k) \cdot W_{\mathrm{cn}}(aK+k) \right) \cdot e^{-j2\pi km/K} + g(m). \end{aligned} \tag{26}$$

The k-th received sub-carrier in the frequency domain can be derived as:

$$R_{\mathrm{Lo}}(k) = X(k) \cdot W_{\mathrm{cn}}(k) + \sum_{a=1}^{\gamma-1} X(aK+k) \cdot W_{\mathrm{cn}}(aK+k) + G_{\mathrm{o}}(k). \tag{27}$$

Thus, the average SINR value of the VC receiver over the Rayleigh fading multipath channel can be expressed as:

$$SINR_{\mathrm{Lo}}(k) = \frac{\mathrm{E}\left[X(k)^2\right] \cdot \mathrm{E}[|W_{\mathrm{cn}}(k)|^2]}{\sigma^2 + \sum_{a=1}^{\gamma-1} \mathrm{E}\left[X(aK+k)^2\right] \cdot \mathrm{E}[|W_{\mathrm{cn}}(aK+k)|^2]}. \tag{28}$$

2) CP Much Shorter Than Combined Response: The major function of the cyclic prefix is that it removes ISI and ICI. In order to address the impact of the case when CP is shorter than the channel response in the VC receiver system, we need to compute both the ISI and ICI noise terms. According to a previous study [18], the ISI and ICI cause interference at the tail of the impulse response. Based on [18], the ISI noise for the VC receiver, in the case that the L_{CP} is shorter than the length (Z) of combined channel and filter impulse response, can be expressed as:

$$N_{\mathrm{ISI}}(k) = \sigma^2 \sum_{c=L_{\mathrm{CP}}+1}^{Z-1} \left|U_c(k)\right|^2, \tag{29}$$

where $U_c(k)$ is defined as:

$$U_c(k) = \sum_{c=L_{\mathrm{CP}}+1}^{Z-1} w_{\mathrm{cn}}(c) e^{-j2\pi ck/N}. \tag{30}$$

Note that the expression for $U_c(k)$ is actually for the FFT of the tail of the combined impulse response. In terms of ICI, [18] shows that the ISI and ICI have the same power spectral density. Therefore, the noise level of ICI is equal to that of the ISI. Thus, the interference power for the VC receiver system can be derived as:

$$\mathrm{E}[N_{\mathrm{So}}(k)^2] = \sigma^2 + \sum_{a=1}^{\gamma-1} \mathrm{E}\left[X(aK+k)^2\right] \cdot \mathrm{E}[|W_{\mathrm{cn}}(aK+k)|^2] + 2\sigma^2 \sum_{c=L_{\mathrm{CP}}+1}^{Z-1} \left|U_c(k)\right|^2. \tag{31}$$

Therefore, the expression of the average SINR for the case where the CP is much shorter than combined response can be written as:

$$SINR_{\mathrm{So}}(k) = \frac{\mathrm{E}\left[X(k)^2\right] \cdot \mathrm{E}[|W_{\mathrm{cn}}(k)|^2]}{\sigma^2 + \sum_{a=1}^{\gamma-1} \mathrm{E}\left[X(aK+k)^2\right] \cdot \mathrm{E}[|W_{\mathrm{cn}}(aK+k)|^2] + 2\sigma^2 \sum_{c=L_{\mathrm{CP}}+1}^{Z-1} \left|U_c(k)\right|^2}. \tag{32}$$

D. Asynchronous ISI Analysis

In the previous sections, we assumed the received signals are perfectly synchronised and sampled at the correct timing. This sub-section will analyse the ISI effects caused by asynchronism. Here we define τ_{Err} as the timing error in samples, which we assume is positive. Thus, interference to the first OFDM symbol $x_1(t)$ is caused by the first τ_{Err} samples from the second OFDM symbol $x_2(t)$. Then, we can write the interference term as:

$$i_{\mathrm{Err}} = \sum_{t=0}^{\tau_{\mathrm{Err}}-1} x_2(t) \otimes b(t). \tag{33}$$

Thus, the interference term on the kth sub-carrier can be rewritten using the Fourier transform as:

$$i_{\mathrm{Err}}(k) = \sum_{k=0}^{N-1} \sum_{n=0}^{\tau_{\mathrm{Err}}-1} X_2(n) B(n) e^{-j2\pi nk/N}, \tag{34}$$

where $X_2(n)$ is the nth FFT output for $x_2(t)$. Then the ISI noise for timing error denoted as N_{IErr}, for the VC receiver with sampling reduction ratio of γ can be derived as:

$$\mathrm{E}\left[N_{\mathrm{IErr}}(k)^2\right] = \sum_{a=0}^{\gamma-1} \sum_{n=0}^{\tau_{\mathrm{Err}}-1} \mathrm{E}\left[X_2(aK+k)^2\right] \cdot \mathrm{E}[|B(aK+k)|^2]. \tag{35}$$

Note that equation (35) represents an extra timing error interference term which can be added to the denominator for our SINR equations to compute the theoretical SINR values when a specified timing error is present.

E. BER Analysis

In terms of comparing the VC receiver BER performance with the standard OFDM receiver system, this paper will use the three BER basic LTE standard modulation schemes, including QPSK, 16-QAM and 64-QAM for both the AWGN channel and the Rayleigh fading multipath channel.

1) Standard OFDM BER Analysis Under the AWGN Channel: The theoretical BER value of the standard OFDM receiver is computed as [19]:

$$\mathrm{BER}_{\mathrm{QPSK}} = \frac{1}{2} \cdot \mathrm{erfc}\left(\sqrt{\frac{E_\mathrm{b}}{N_\mathrm{o}}}\right), \tag{36}$$

$$\mathrm{BER}_{16-\mathrm{QAM}} \approx \frac{3}{8} \cdot \mathrm{erfc}\left(\sqrt{\frac{2}{5} \cdot \frac{E_\mathrm{b}}{N_\mathrm{o}}}\right), \tag{37}$$

$$\mathrm{BER}_{64-\mathrm{QAM}} \approx \frac{7}{24} \cdot \mathrm{erfc}\left(\sqrt{\frac{1}{7} \cdot \frac{E_\mathrm{b}}{N_\mathrm{o}}}\right), \tag{38}$$

where $\mathrm{erfc}(.)$ denotes the complementary error function. The relationship between $E_\mathrm{b}/N_\mathrm{o}$ and $SINR$ can be presented as:

$$E_\mathrm{b}/N_\mathrm{o} = \frac{\overline{SINR}}{N_\mathrm{bs}}, \tag{39}$$

where N_bs is the number of bits per sample.

2) Standard OFDM BER Analysis Under the Rayleigh Multipath Channel: The theoretical BER value of normal OFDM system over the Rayleigh multipath channel is computed as [19] [20]:

$$P_{\mathrm{QPSK}} = \frac{1}{2}\left(1 - \sqrt{\frac{E_\mathrm{b}/N_\mathrm{o}}{1 + E_\mathrm{b}/N_\mathrm{o}}}\right), \tag{40}$$

$$P_{16-\mathrm{QAM}} = \frac{1}{2}\left(1 - \frac{3}{4}\sqrt{\frac{4 \cdot E_\mathrm{b}/N_\mathrm{o}}{5/2 + 4 \cdot E_\mathrm{b}/N_\mathrm{o}}} - \frac{1}{2}\sqrt{\frac{4 \cdot E_\mathrm{b}/N_\mathrm{o}}{5/18 + 4 \cdot E_\mathrm{b}/N_\mathrm{o}}} + \frac{1}{4}\sqrt{\frac{4 \cdot E_\mathrm{b}/N_\mathrm{o}}{1/10 + 4 \cdot E_\mathrm{b}/N_\mathrm{o}}}\right). \tag{41}$$

For the 64-QAM modulation, the BER expression is:

$$P_{64-\mathrm{QAM}} = \sum_{i=1}^{28} \omega_i I(a_i, b_i, \overline{\gamma}, r, \rho), \tag{42}$$

TABLE I

COMMON SIMULATION PARAMETERS

Simulation Parameters						
Bandwidth	N	Transmitted f_s	L_{CP}	IIR Filter Order	Type of Filter	Attenuation
20 MHz	2048	30.72 MHz	144	4	Butterworth	3 dB
Filter Impulse Response						
Filter Parameters (γ)	1/2	1/4	1/8	1/16	1/32	1/64
Approximate FIR Filter Length (L_F)	24	35	67	132	208	332

where $\overline{\gamma}$ is the average SNR per symbol and coefficients ω_i, a_i, b_i are listed in a table in [21] and I is the integral representation:

$$I(z) = \frac{1}{\pi} \int_{-(\pi/2)}^{(\pi/2)} e^{-z \cdot \sin\phi} d\phi. \tag{43}$$

V. Simulation Results

This section will firstly evaluate the bandwidth efficiency performance and the energy saving performance by using the VC receiver system rather than a full bandwidth OFDM receiver. Then theoretical and simulation results for the SINR and BER performance will be described. Common parameters for simulations are listed in Table I.

A. LTE Downlink Efficiency Performance

The result for the LTE downlink capacity for one 10 ms LTE radio frame with the number of PDCCH transmissions is shown in Fig. 4. The LTE bandwidth efficiency is computed as Equation (11) and it is obvious that whether one or two PDCCH symbols is used, the percentage capacity of 20MHz bandwidth is much higher than other options, and the least efficient is the 1.4MHz

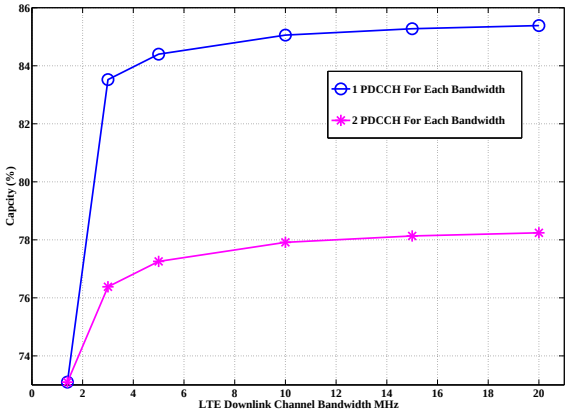

Fig. 4. LTE Downlink Capacity Vs. Channel Bandwidth

TABLE II

ENERGY SAVING PERFORMANCE OF THE VC SYSTEM FOR THE 20MHZ LTE CHANNEL FROM EQUATIONS (14) AND (15)

Sampling Rate (f_s)	FFT Size (N)	Normalised ADC Power (W)	FFT Computational Complexity (Ops)
30.72MHz	2048	1	11264
15.36MHz	1024	1/2	5120
7.68MHz	512	1/4	2304
3.84MHz	256	1/8	1024
1.92MHz	128	1/16	448
0.96MHz	64	1/32	192

bandwidth carrier. We can conclude that compared with the SP and CA methods, using a virtual carrier mapped into a 20MHz LTE band can improve bandwidth efficiency significantly.

B. Energy Saving Performance for the VC Receiver

Compared with the 20 MHz LTE standard receiver, the ADC dissipation performance and the computational complexity of the FFT block for the virtual carrier receiver system is shown in Table II. In order to compare the cost-efficiency, we defined the energy cost of processing the full 20 MHz bandwidth to be normalised to 1. By reducing the sampling rate of a M2M receiver, the ADC power dissipation and the computational complexity are reduced significantly. If a M2M terminal device only needs to decode 64 sub-carriers, by using a low pass filter and sampling rate at 0.96 MHz, it only costs 1/32 of the ADC operations compared with decoding the whole 20 MHz band and the FFT computation is reduced from 11264 operations to 192.

C. SINR Performance

The SINR performance of the VC receiver system over the AWGN channel with four types of IIR analogue filter (Butterworth, Chebyshev I, Chebyshev II and Elliptic filters [22]) with $\gamma = 8$ is shown in Fig. 5. The passband ripple for Chebyshev I is set to 1dB and the stopband ripple for Chebyshev II is set to 40dB. In the case of the Elliptic filter, the passband and stopband ripple are set to 1dB and 40dB in order to provide fair comparison. We plot the SINR value for the first 128 sub-carriers in Fig. 5 and it shows that the sub-carriers near the cut-off frequency band present significant SINR loss. It also shows that both the Butterworth and the Chebyshev I filters achieve higher SINR performance in the passband compared with Chebyshev II and Elliptic filters. However, the Chebyshev I filter has a worse phase response because of group delay variations at the band edges. Therefore, in order to achieve a high SINR performances in the pass band frequency, this paper will focus on the Butterworth IIR filter in the remaining simulations.

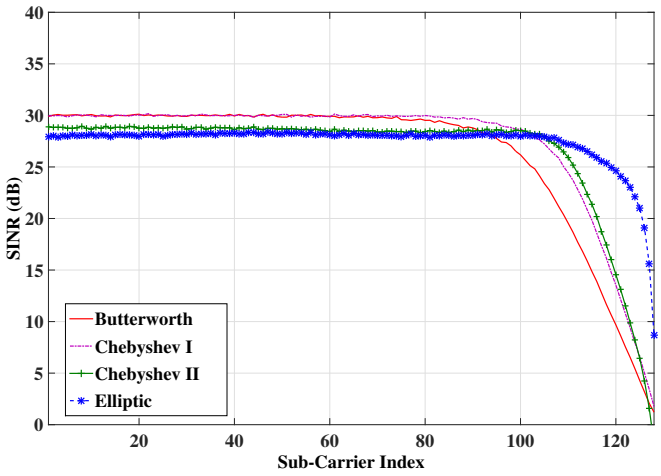

Fig. 5. SINR Performance over Different IIR Filters, AWGN channel 30dB, $N = 2048$, $L_{\mathrm{CP}} = 144$, $\gamma = 8$, 16-QAM.

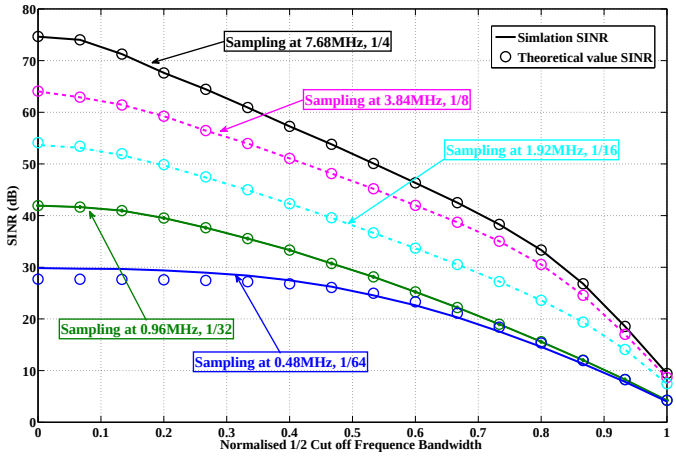

Fig. 6. SINR Performance for Different Sampling Rate, $G_{\mathrm{o}} = 0$, $h_i = 0$, $N = 2048$, $L_{\mathrm{CP}} = 144$, 16-QAM.

The SINR performance for different sampling reduction ratios is shown in Fig. 6 with the assumption of a 16-QAM modulation scheme and no background noise, and there is perfect time synchronisation. When γ is 64, L_{F} is much larger than L_{CP}. Thus we computed the ISI and ICI noise power using equation (31) for $\gamma = 64$ to obtain the theoretical value of the SINR which is

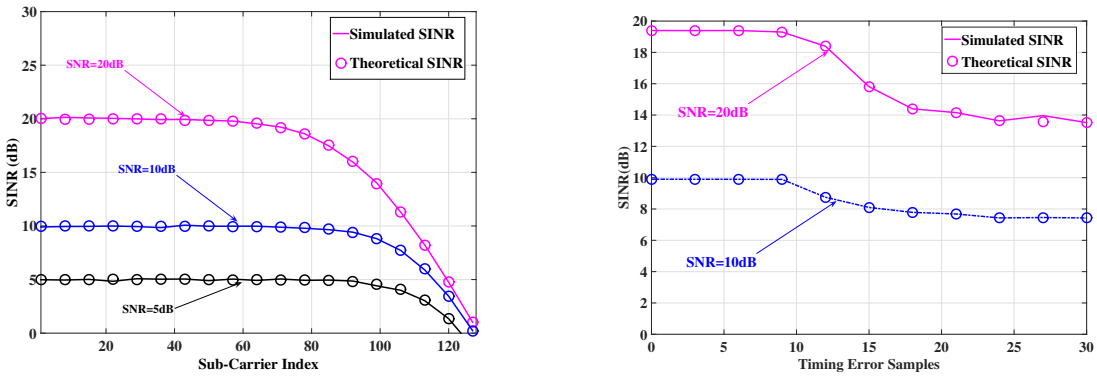

(a) None Timing Error (b) With Timing Error

Fig. 7. SINR Performance over the AWGN channel, Butterworth, QPSK, $N = 2048$, $L_{\mathrm{CP}} = 144$, $\gamma = 8$.

computed from equation (23). The theoretical results show a perfect match with the simulations. If the M2M receiver samples at 0.48 MHz (about 1/64 of transmitted sampling rate, the IIR cut-off frequency is set to 0.3125 MHz in order to match with the sampling reduction ratio), the SINR value of the first 65% of all sub-carriers is still above 20dB. It also indicates that the VC receiver system is able to decode the transmitted low data rate M2M messages mapped into a normal LTE band, even if we reduced the sampling rate by 64 times. The basic reason for the SINR performance with $\gamma = 32$ and $\gamma = 64$ being much poorer than other cases is the non-integer sampling reduction of the CP.

The SINR degradation performance of the VC receiver system without timing error over the AWGN channel is shown in Fig. 7(a). The transmitted SNR is set to 20dB, 10dB and 5dB. The theoretical SINR value is computed using (25) and it is closely matched with simulations. The AWGN channel does not significantly affect the SINR performance of the VC receiver. If the input SNR is 20dB, the SINR degradation becomes apparent at sub-carrier number 80, where there is about 2dB SINR loss. By reducing the transmitted SNR, the SINR degradation in the

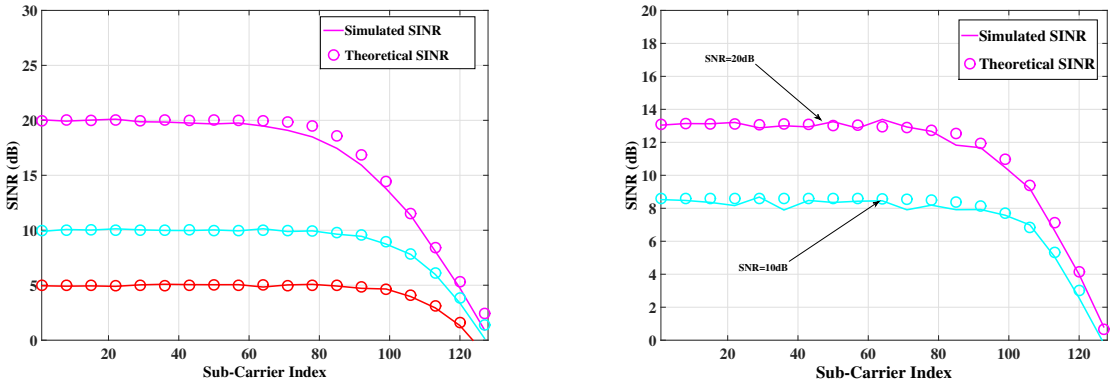

(a) SINR for Channel Taps: 20

(b) SINR for Channel Taps: 300

Fig. 8. SINR Degradation Caused by a Rayleigh Fading Channel, Butterworth, QPSK, $N = 2048$, $L_{\mathrm{CP}} = 144$, $\gamma = 8$.

VC receiver mores closer to half the cut-off frequency. In terms of the first 60-70 sub-carriers, the VC receiver system presents high SINR performance. The SINR performance versus timing error τ_{Err} is shown in Fig. 7(b). The ISI of timing error is computed using (35), and added to the denominator of (25) to compute the theoretical SINR, which perfectly matches the simulations. When τ_{Err} is larger than 9 samples, the SINR performance is significantly reduced.

The SINR degradation performance over the Rayleigh multipath channel is shown in Fig.8. Assuming the VC receiver has received the signal over a $J = 20$ tap Rayleigh fading channel, the length of CP is longer than the combined impulse response and the ADC sampling follows perfect timing, the SINR performance is shown in Fig.8(a). The theoretical value of the SINR is computed using equation (28), and similar to the AWGN channel case, the Rayleigh fading channel does not significantly affect the average SINR in the passband. Now we increase the length of channel to 300 taps i.e. the ”long channel”. Thus, the CP is not long enough to prevent ISI and ICI interference as shown in Fig. 8(b), where the theoretical value is computed using equation (32). It is obvious that there is a significant SINR degradation in the passband due to

the ISI and ICI. For a received signal with 20dB SNR over a 300 tap multipath channel, the average SINR of the down-sampled signal is reduced to 13dB in the passband. Therefore, the performance of the VC receiver can be limited by increases in the number of channel taps J.

D. BER Performance

In terms of testing the BER performance of the VC receiver system, we assume the transmitted M2M messages are mapped in to the first 90 sub-carriers over a 20 MHz LTE channel. According to Fig. 7(a), the SINR values of sub-carriers 1-90 would not be affected significantly by using sampling reduction ratio of $\gamma = 8$. Therefore, in this section, we will examine the BER performances of sub-carriers from 1 to 90.

The BER performance of the VC receiver over the AWGN channel is shown in Fig. 9(a), we compared the theoretical value of the normal OFDM system derived from equation (36) - (38) and the simulated value of the VC system. It is obvious that the VC receiver system can achieve the same BER performance compared with the traditional LTE receiver even when reducing the receiver ADC sampling rate. The BER performance of the Rayleigh fading channel is shown in Fig. 9(b). The BER performance of the VC receiver system is closely matched with the normal OFDM receiver performance obtained from equation (40) - (42). There are slightly higher BER values for E_b/N_0 between 25dB to 30dB. The reason for that is the VC receiver system causes a small SINR degradation around sub-carrier 90, especially for high input SNR. However, the VC receiver system still can perfectly decode the transmitted low data rate M2M messages without significant BER degradation by using only 1/8 of the ADC power and reducing the computational complexity from 11264 operations to 1024.

In order to measure the BER performance of the VC receiver affected by both ISI and ICI, this paper increased the multipath Rayleigh fading channel taps 200, 300 and 500 with $L_{\mathrm{CP}} = 144$

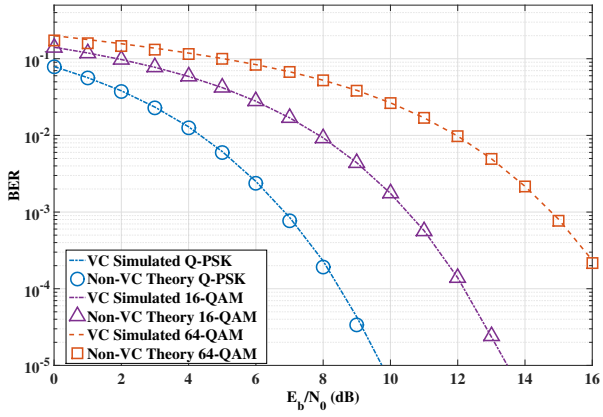

(a) BER Performance of the Virtual Carrier System over the AWGN Channel

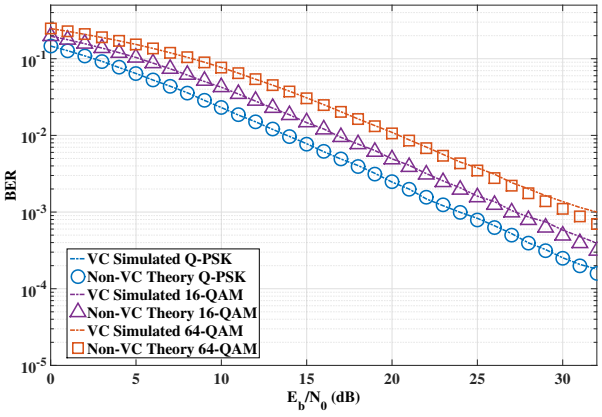

(b) BER Performance of the Virtual Carrier System over the Rayleigh fading Channel, Channel Taps=20

Fig. 9. BER Performance of VC Receiver System, Butterworth, $N = 2048$, $L_{\mathrm{CP}} = 144$, $\gamma = 8$.

and the result is shown in Fig. 10. The theoretical BER value is computed by substituting the SINR value from equation (32) into equation (41), which closely matches with simulations. It clearly indicates that by increasing the number of channel taps, the BER degradation will increase significantly due to the presence of ICI and ISI. When the channel taps increased to 500, the gap between the OFDM system and the VC system becomes small. This means the CP is no longer to protect the received signal against ICI and ISI. Compared with the standard OFDM receiver, the VC receiver is more sensitive to the number of channel taps J. Therefore, the VC receiver system might not suitable for some very bad channel conditions, so future studies might focus on how to reduce the ISI and ICI effects while at the same time reducing the cost of the receiver.

VI. Conclusion

In this paper, a practical virtual carrier receiver system is proposed that uses a narrow band analogue filter and a much lower sampling rate ADC in order to extract the low data rate

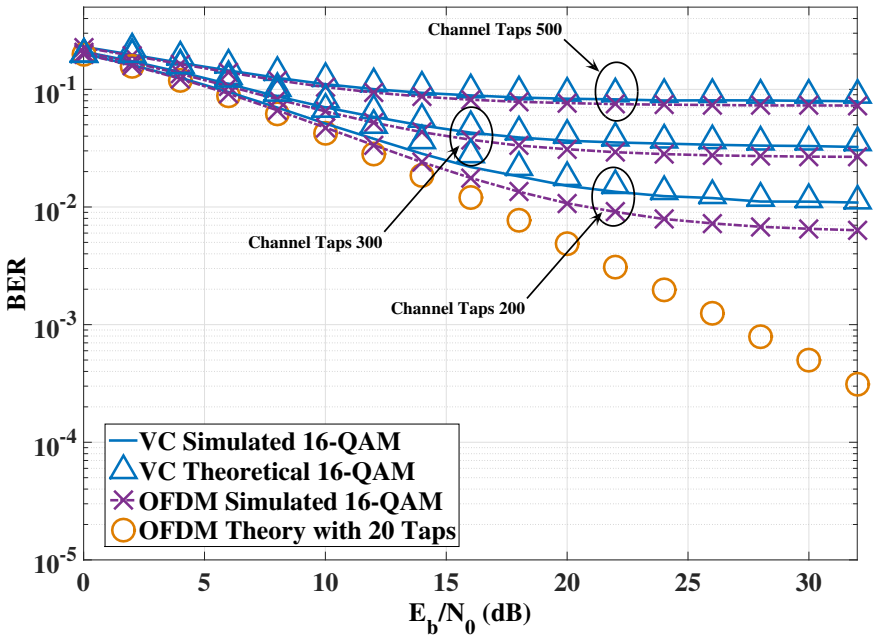

Fig. 10. BER Performance over a much longer Rayleigh flat fading multipath channel, 16-QAM, $\gamma = 8$, $L_{\mathrm{CP}} = 144$.

M2M signals while significantly reducing the ADC power consumption and the computational complexity. In order to modify the existing LTE communication systems to support low data rate M2M devices, the VC receiver can significantly improve the LTE bandwidth efficiency and cost-efficiency. At the same time, it provides high SINR and BER performance close to a full sample rate OFDM receiver for the sub-carriers of interest. Secondly, this paper has derived the theoretical analysis of the VC receiver performance, which perfectly match with simulations. The theoretical equations account for the effect of aliasing spread on the sub-carrier location, and this helps to the system designer to evaluate what kind of filters and receiver sampling rate can be used to balance the energy cost and detection performance. This paper highlights that the VC receiver system could be a suitable solution to support the M2M communications based on the LTE standard.

REFERENCES

[1] M. F. L. Abdullah and A. Z. Yonis, "Performance of LTE Release 8 and Release 10 in wireless communications," in *CyberSec. Conf.*, 2012, pp. 236–241.

[2] *3GPP TR 36.888, Study on Provision of Low-Cost Machine-Type Communications (MTC) User Equipments (UEs) Based on LTE*.

[3] H. S. Dhillon, H. C. Huang, H. Viswanathan, and R. A. Valenzuela, "Power-efficient system design for cellular-based machine-to-machine communications," *IEEE Trans. Wireless Commun.*, vol. 12, no. 11, pp. 5740–5753, November 2013.

[4] N. Michailow, M. Matthe, I. Gaspar, A. Caldevilla, L. Mendes, A. Festag, and G. Fettweis, "Generalized frequency division multiplexing for 5th generation cellular networks," *IEEE Trans. Commun.*, vol. 62, no. 9, pp. 3045–3061, Sept 2014.

[5] R. Lu, X. Li, X. Liang, X. Shen, and X. Lin, "GRS: The green, reliability, and security of emerging machine to machine communications," *IEEE Commun. Mag.*, vol. 49, no. 4, pp. 28–35, April 2011.

[6] D. Niyato, L. Xiao, and P. Wang, "Machine-to-machine communications for home energy management system in smart grid," *IEEE Commun. Mag.*, vol. 49, no. 4, pp. 53–59, April 2011.

[7] M. Beale, "Future challenges in efficiently supporting M2M in the LTE standards," in *WCNC Workshops*, 2012, pp. 186–190.

[8] S. Wang and J. Thompson, "Signal processing implementation of virtual carrier for supporting M2M systems based on LTE," in *IEEE Vehicular Technology Conference (VTC Spring)*, May 2015, pp. 1–5.

[9] S.-E. Elayoubi, O. Ben Haddada, and B. Fourestie, "Performance evaluation of frequency planning schemes in OFDMA-based networks," *IEEE Trans. Wireless Commun.*, vol. 7, no. 5, pp. 1623–1633, May 2008.

[10] E. Au, C. Wang, S. Sfar, R. Murch, W.-H. Mow, V. Lau, R. Cheng, and K. Letaief, "Error probability for MIMO zero-forcing receiver with adaptive power allocation in the presence of imperfect channel state information," *IEEE Trans. Wireless Commun.*, vol. 6, no. 4, pp. 1523–1529, April 2007.

[11] K. Pedersen, F. Frederiksen, C. Rosa, H. Nguyen, L. Garcia, and Y. Wang, "Carrier aggregation for LTE-Advanced: functionality and performance aspects," *IEEE Commun. Mag.*, vol. 49, no. 6, pp. 89–95, June 2011.

[12] B. Widrow, I. Kollar, and M.-C. Liu, "Statistical theory of quantization," *IEEE Trans. Instrum. Meas.*, vol. 45, no. 2, pp. 353–361, Apr 1996.

[13] M. K. C. Gessner, A. Roessier. (2012, July) UMTS long term evolution (LTE) - technology introduction application note. 3GPP. [Online]. Available: http://cdn.rohde-schwarz.com/pws/dl_downloads/dl_application/application_notes/1ma111/1MA111_4E_LTE_technology_introduction.pdf

[14] LTE resource grid. LG Space. [Online]. Available: http://niviuk.free.fr/lte_resource_grid.html

[15] T. Sundstrom, B. Murmann, and C. Svensson, "Power dissipation bounds for high-speed nyquist analog-to-digital converters," *IEEE Trans. Circuits Syst. I, Reg. Papers*, vol. 56, no. 3, pp. 509–518, March 2009.

[16] K. Parhi and M. Ayinala, "Low-complexity Welch power spectral density computation," *IEEE Trans. Circuits Syst. I, Reg. Papers*, vol. 61, no. 1, pp. 172–182, Jan 2014.

[17] B. Mulgrew, P. Grant, and J. Thompson, *Digital Signal Processing: Concepts and Applications*, 2nd Edition edition, Ed. Palgrave Macmillan, 2002.

[18] W. Henkel, G. Taubock, P. Odling, P. Borjesson, and N. Petersson, "The cyclic prefix of OFDM/DMT - an analysis," in *in Proc. Inremotional Seminar on Broadbond Communicalions, Access, Trommission, Networking, Zurich*, 2002, pp. 22–1–22–3.

[19] J. Thompson and A. Smokvarski, "Bit Error Ratio performance of a receiver diversity scheme with channel estimation," *IET Communications*, vol. 1, no. 1, pp. 92–100, February 2007.

[20] F. Adachi, "BER analysis of 2PSK, 4PSK, and 16QAM with decision feedback channel estimation in frequency-selective slow rayleigh fading," *IEEE Trans. Veh. Technol.*, vol. 48, no. 5, pp. 1563–1572, Sep 1999.

[21] X. Tang, M.-S. Alouini, and A. Goldsmith, "Effect of channel estimation error on M-QAM BER performance in rayleigh fading," *IEEE Trans. Commun.*, vol. 47, no. 12, pp. 1856–1864, Dec 1999.

[22] R. Losada and V. Pellisier, "Designing IIR filters with a given 3-db point," *IEEE Signal Process. Mag.*, vol. 22, no. 4, pp. 95–98, July 2005.